

Visualization of the turbulent states transition in GYM plasmas using fast imaging

D.Iraji¹, D.Ricci¹, A.Cremona¹, S.Garavaglia¹, G.Granucci¹, D.Minelli¹

¹*Istituto di Fisica del Plasma, CNR, Milano, Italy*

Abstract

In the GYM linear magnetized plasma device electrostatic probe measurements and time resolved emissivity profiles of the plasma column are used to investigate turbulence state transition in different plasma conditions obtained by changing the injected microwave power, the axial magnetic field and hydrogen gas pressure. To perform a statistical, temporal and spatial analysis of turbulent structures, an object tracking method has been developed which detects, follows and registers plasma blobs in the camera data. Information on the blobs such as size and speed have been used to perform statistical analyses which show presence of phase transition between different classes of turbulent structures in terms of their speeds and sizes.

Introduction: Characterization of turbulence is an important research line in all kinds of plasma machines including basic plasma devices. Basic plasma devices provide a wide range of plasma control parameters and accessibility to investigate plasma turbulence and its associated transport [1, 2]. Fast framing cameras as a non-perturbative diagnostic provide acceptable spatial-temporal resolution to study turbulence and are widely used among different plasma research groups [3-6]. In the GYM linear magnetized plasma device, low frequency electrostatic fluctuations are measured by means of Langmuir probes as well as a non-perturbative imaging system [7]. Analyses showed that in GyM plasmas, fluctuations are mainly derived by $E \times B$ drift mechanism [8], while the camera data also show presence of fast structures or blobs. In this work, in order to investigate these fast blobs, the camera data are used to perform statistical, temporal and spatial analysis by tracking blobs in different plasma conditions which are obtained by changing injected microwave power, axial magnetic field and hydrogen gas pressure.

Experimental setup: This work has been performed on the GyM device that has length $L = 211\text{cm}$, radius $a = 12.5\text{cm}$ and axial magnetic field B up to 100 mT. Highly reproducible plasmas are sustained in CW mode by means of electromagnetic waves at the electron cyclotron frequency of 2.45 GHz using a magnetron with power up to 2.0 kW. Fig. 1 shows schematic view of GyM vacuum chamber (red rectangle) super imposed by the magnetic field map for the coil current of 600A. Contours indicate electron cyclotron resonance (EC) layers that acts as a

plasma source inside the chamber. A metallic grounded ring (shown as thick black bars in Fig. 1) is placed inside the vacuum chamber which limits plasma into a cylindrical column with diameter of $d=12.5$ cm around the axis of the machine.

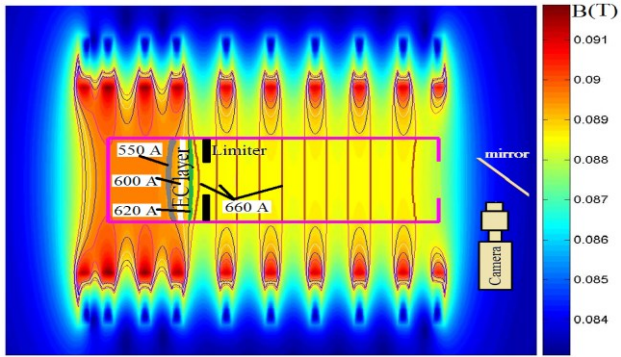


Fig.1: Schematic view of the vacuum chamber (pink rectangle) and the calculated magnetic field map for coil current of 600A.. The bold gray, white and green lines inside the rectangle represent the EC resonance layers corresponding to the coil current values of 550, 600 and 620A, respectively. In the case of 660A, there are multiple EC resonance layers (brown lines) inside the chamber.

Because of the magnetic field coils arrangement in GyM, the position of the plasma source depends on the coils current. There are two high and low magnetic field regions inside the vacuum chamber (Fig.1) which respectively can be called ‘source region’ (left hand side of the limiter) and ‘source free region’ (right hand side of the limiter). The coil currents are varied in the range of 550 – 620 A to avoid the complexity of having multiple plasma sources in the source free region. This corresponds to a variation of the axial magnetic field in the source free region in the range of 73 – 82 mT. Therefore, different plasma conditions, obtained with six levels of microwave power (MP) in the 500 – 1750 W range, five values of axial magnetic field and three values of hydrogen pressure in the range of $2 \times 10^{-4} – 5 \times 10^{-4}$ mbar corresponding to neutral gas densities of $n_N \sim 6 \times 10^{18} \text{ m}^{-3}$, $8 \times 10^{18} \text{ m}^{-3}$ and $13 \times 10^{18} \text{ m}^{-3}$) are considered to investigate characteristics of turbulent structures such as their sizes and speeds. In this work, the fast camera data are acquired for 200 ms at 100 kframes/s with $2\mu\text{s}$ of exposure time. Besides the fast imaging system a radially movable 8-tips Langmuir probe array is used to measure electron density and temperature in the range of $2\text{cm} < r < 11\text{cm}$, where r is the radial distance from the axis of the chamber. Emissivity fluctuations in the camera images are commonly used to perform Fourier analysis, two point correlation and conditional average sampling [5]. All these techniques give information about coherent structures that last for a long time compared to the temporal resolution of the camera data which, in this work, is $10 \mu\text{s}$. Short life time fluctuations which appear only in few consecutive frames are averaged out and are neglected. In order to investigate short life time/fast blobs, a structure tracking method has been developed which detects and follows plasma blobs in consecutive frames of the camera data. The detected blobs

with minimum face size of 3 pixels and minimum life time of 2 frames are registered in a file. The registered blobs file provides information about temporal evolution of the face size, peak value/position, center of mass value/position and speed of each detected blob. As an example, in Fig. 2, four consecutive frames show movement of a tracked blob. Pixels of the blob are marked with “+” signs. Face size of each blob is calculated using pixel calibration factor. In this work, radius of the best fitted circle to each registered blob is considered as blob size. Statistical analyses of the blobs size and speed open an insight to the collective behavior of plasma structures as well as their individual behavior in different conditions [9-11]. Therefore, the structure tracking technique has been applied to camera data corresponding to different plasma conditions obtained by changing the microwave power, magnetic field and neutral gas density.

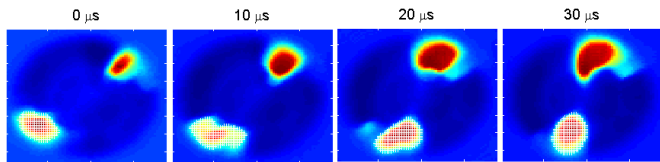


Figure 2 Four Consecutive camera frames showing movement of one detected blob. “+” represent corresponding pixels to the tracked blob.

Results: Fig. 3 and Fig. 4 respectively show probability distribution function (PDF) of blob size and blob speed in different plasma conditions ($MP=480W$ to $1800W$, $B\sim 73mT$, $n_N\sim 6\times 10^{18} m^{-3}$). Similarly, PDFs of blob size and speed are calculated for all combinations of MP , B and n_N from the corresponding registered blobs. The probe array measurements have been used to calculate the mean values of the electron density and the electron density gradient, which are obtained by averaging over $2cm < r < 11cm$. In order to investigate relation between the electron density profile and blob size, for each set of MP , B and n_N , $L_{n_e}^{-1} = \frac{\nabla n_e}{n_e}$ is calculated from the corresponding electron density profile and $blob\text{-size}_{mean}$ is obtained from the PDF of blob size ($blob\text{-size}_{mean}$ is the mean value of blob sizes). In Fig.5.a values of $blob\text{-size}_{mean}$ are plotted with respect to the corresponding $L_{n_e}^{-1} = \frac{\nabla n_e}{n_e}$. Different colors correspond to different values of B . Fig. 5 (b) shows the joint probability between size and speed of all tracked blobs.

Discussion: As shown in Fig. 3, 4, for given values of B and n_N , distributions of blob size vary with MP . The peak of the blob size distribution shifts toward small sizes as MP increases, while the blob speed distribution remains mainly unchanged.

In Fig. 5.a blob-size_{mean} decreases by increase of $L_{n_e}^{-1}$. Fig. 5.b shows the joint probability between sizes and speeds of all tracked blobs. There are different groups of blobs in terms of size and speed which represent different turbulent state. Transitions between these turbulent states can be achieved by applying particular combinations of B, MP and n_N.

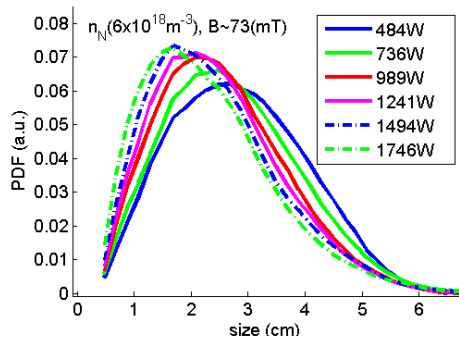


Figure 3 Probability distribution function of blob face size for different microwave powers (480W to 1240W) at $B \sim 73$ mT and neutral gas density $n_N \sim 6 \times 10^{18} \text{ m}^{-3}$.

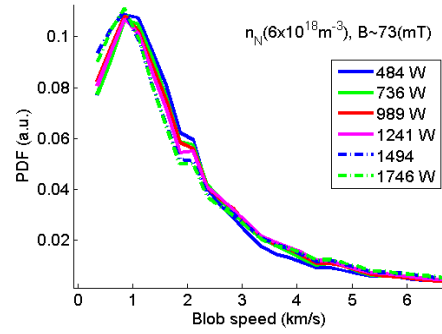


Figure 4 Probability distribution function of blob speed size for different microwave powers (480W to 1240W) at $B \sim 73$ mT and neutral gas density $n_N \sim 6 \times 10^{18} \text{ m}^{-3}$.

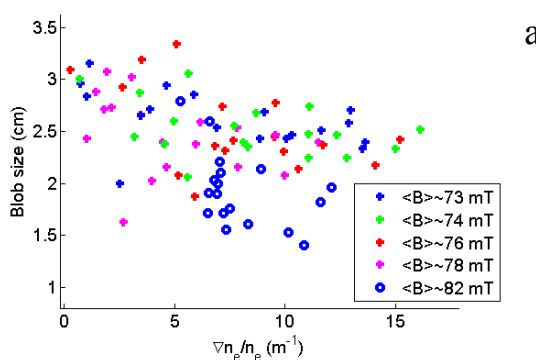
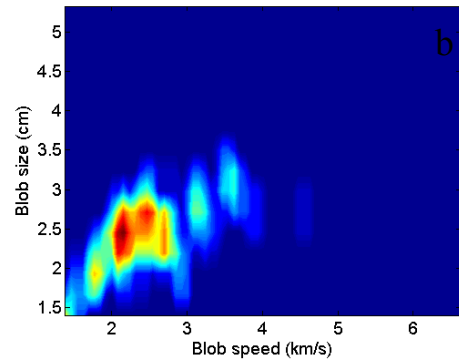


Figure 5 (a). Variation of blob size mean value vs $L_{n_e}^{-1} = \frac{\nabla n_e}{n_e}$, for B values ranging from 73 to 82 mT, injected microwave power from 480 to 1800W, and the neutral gas densities of $n_N \sim 6 \times 10^{18} \text{ m}^{-3}$, $8 \times 10^{18} \text{ m}^{-3}$ and $13 \times 10^{18} \text{ m}^{-3}$. (b). Joint probability between size and speed of all tracked blobs. Each high probability region represents one group of blobs in terms of blob size and speed.



- [1] E.J.Doyle, et.al, Nucl. Fusion **47**, S18 (2007).
- [2] J.A.Boedo, et.al, Physics of Plasmas **8**, 11 (2001).
- [3] S.J.Zweben, et.al, Nucl.Fusion **44**, 134 (2004).
- [4] G.Y.Antar, et.al, Phys.Rev.Lett **87**, 6 065001 (2001).
- [5] D. Iraji, I. Furno, A. Fasoli, C. Theiler, Physics of Plasmas, **17** 122304, 2010.
- [6] D. Iraji, I. Furno, A. Fasoli, IEEE Transactions on Plasma Physics, **39**, no.11, page 3010,
- [7] G.Granucci et.al., 36th EPS, ECA Vol.**33E**, P-4.148 (2009).
- [8] D. Iraji, D. Ricci, G. Granucci, et.al, Fusion Science and Technology, 62, 2012.
- [9] I. Furno, C.Theiler, D. Lancon, et.al, Plasma Physics and Controlled Fusion, **53** 124016, 2011.
- [10] C. Theiler, I. Furno, A. Fasoli, P. Ricci, et.al Physics of Plasmas **18**, 055901 2011.
- [11] B.Labit,et.al, Phys.Rev.Lett **98**, 255002 (2007).